Supplement of

Assessing atoll island future habitability in the context of climate change using Bayesian networks

This supplement details the method developed in this paper to convert scores and confidence levels into probabilities (S1). It also includes the complementary results of the Bayesian network (BN) analysis (S2) and the sensitivity test applied to the BN (S3).

S1. Expert judgments into probabilities

This supplement supports section 2.4.2 of the main manuscript.

In this study, we used the risk assessment database from (Duvat et al., 2021) as input data. This database is available in the supplement provided by (Duvat et al., 2021) and it contains the risks and confidence levels evaluated by the experts. To populate the conditional probability tables, we converted the risk and confidence levels into probability distributions. For each combination of risk level – confidence level, we generated a conditioned Beta distribution. This is detailed in the next sections.

S1.1. Beta distribution

The Beta distribution is a continuous probability distribution defined on the interval [0, 1]. The shape of the distribution is determined by two parameters usually denoted α and β Eq. S1:

$$Beta(\alpha, \beta) = \frac{p^{\alpha-1}(1-p)^{\beta-1}}{B(\alpha,\beta)}, \quad \text{(S1)}$$

The Beta distribution is useful to model the uncertainty of a probability value p, based on prior knowledge about p. Figure S1 shows some examples of Beta distributions with different values of α and β. To represent how α and

β define the shape of the distribution, we can consider α as the number of successes and β *as* the number of failures. When both parameters are set to one, we obtain a uniform distribution. This would mean that there is no prior information about p, therefore, it is equally likely to take all values between 0 and 1. When α increases, the bulk of the distribution shifts rightward, this indicates a higher probability of success p with more observed successes. Conversely, when β increases (observed failures), the probability of success decreases. This results in a leftward shift of the bulk of the distribution. When both α and β increase, the distribution gets narrower, indicating a greater amount of information and less uncertainty about p.

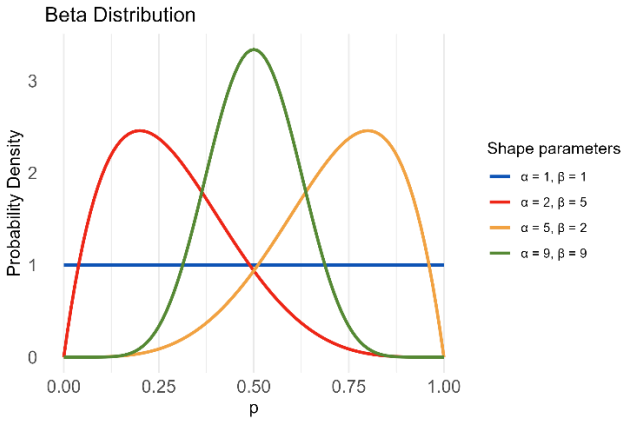

Figure S1 Use of the Beta distribution in this study.

In this work, we translated expert judgments into probabilities to populate the conditional probabilities tables. Our objective was to define a probability distribution that describes risk and confidence levels assessed by (Duvat et al., 2021). To do this, we selected the Beta distribution because its mathematical properties are suited well to our problem. These properties include the finite support and the flexibility to represent different families of probability distributions.

We generate a Beta distribution for each combination of assessed risk and confidence levels satisfying the following conditions:

- Condition 1) the mode (peak of the distribution) corresponds to the risk level assessed by the experts, to ensure that the risk level assessed by the experts has the highest probability. The probability of the mode varies depending on the confidence level, a higher confidence results in a higher probability.
- Condition 2) the standard deviation (the spread of the probabilities) depends on the confidence level. We associated a higher confidence with a lower spreading.

To satisfy the first condition, we associated a probability weight with each confidence level. For a confidence level of one, we considered a very low degree of certainty, and we assigned a probability of 30% to best guess risk level. With a confidence level of two, we considered a low degree of certainty, and the probability of the best guess risk level was set at 40%. Thus, for a moderate, high, and very high confidence level, we set the probability of the best guess risk level at 60%, 80% and 100%, respectively. To represent the higher confidence level we used a Dirac distribution.

We selected the weights after several tests. Our test results showed that a confidence level associated with a probability of the best guess risk level that is lower than 30% leads to a loss of information. Conversely, a

probability higher than 30% results in narrower distributions that could overfit the model. We also considered that a probability higher than 30% was too high to be associated with a very low confidence level.

The second condition dictates how the probabilities are assigned to risk levels not corresponding to the best guess. In Duvat et al. (2021), the experts conducted a risk assessment with an associated degree of uncertainty. Therefore, there is a probability that the risk estimated by the experts may be higher or lower than predicted. To reflect this probability, we associated each confidence level with a specific standard deviation. A lower confidence level was associated with greater uncertainty, and therefore this was represented by a higher value of standard deviation (Table S1). Conversely, a higher degree of confidence was associated with a narrower spread and therefore with a lower value of standard deviation.

Table S1 Probability weight and standard deviation associated with a confidence level.

Confidence level	Probability weight	Standard deviation
1	30%	0.25
2	40%	0.20
3	60%	0.15
4	80%	0.10
5	100% (Dirac)	-

To generate the Beta distributions we determined the shape parameters using optimization functions. These functions used the BFGS (Broyden-Fletcher-Goldfarb-Shanno) algorithm to find α and β values that fit better to our previous conditions.

The first optimization function finds the combination of α and β that best satisfies the standard deviation condition (Table S1). The second function uses the found α and β values as the initial parameters to find a new combination of α and β that best satisfies the probability weight condition (Table S1). A third function is used to correct the asymmetry of the distributions. Despite this last correction, some distributions remain slightly asymmetric. However, this skewness does not produce significant changes in the results.

We used different combinations of shape parameters to create fifteen Beta distributions, one for each risk level and confidence level (Figure S2). Finally, we used the beta distributions to populate the conditional probability tables as shown in Figure S3.

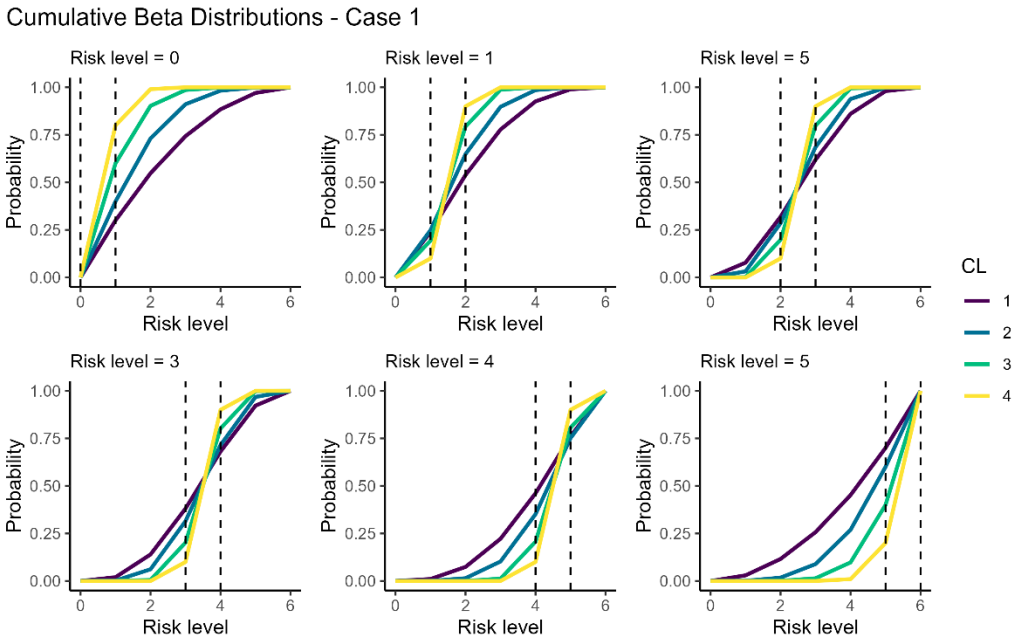

Figure S2 Beta distributions generated for each risk level and confidence level. The support of the distribution was divided into 6 intervals, one for each risk level. The dotted lines indicate the probability interval corresponding to each risk level.

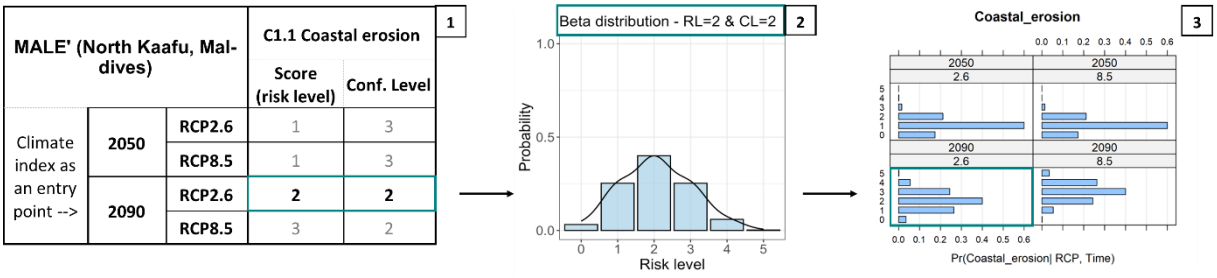

Figure S3 Steps to convert expert judgments into probabilities. For each combination risk-confidence level (1) we generated a Beta distribution (2). The probabilities were then used to populate the conditional probability tables (3).

S2. BN analysis results for all atoll islands

This supplement supports sections 4.1, 4.2, 4.3, and 4.4 of the main manuscript.

S2.1. Identification of critical thresholds: What levels of risk could lead to adaptation limits?

In this analysis, we explored the possibility for islands to reach adaptation limits. To do this, we interrogated the model to determine in which conditions specific thresholds can be exceeded. Figure S4 illustrates the outcomes for Tabiteuea and Nolhivaranfaru under RCP 8.5 in 2090. In both atoll islands, the results suggest that severe risk criteria (levels 4 or 5) may lead to exceeding this threshold. This analysis also allows to identify the risk criteria with the major contribution to the risk to habitability. This is reflected by the magnitude of the distribution shift. In both atoll islands, variations on the risk level of *loss of settlements* generate a slight distribution shift and therefore a slight impact on habitability. In contrast, increments in *flooding* risk level have a more important contribution.

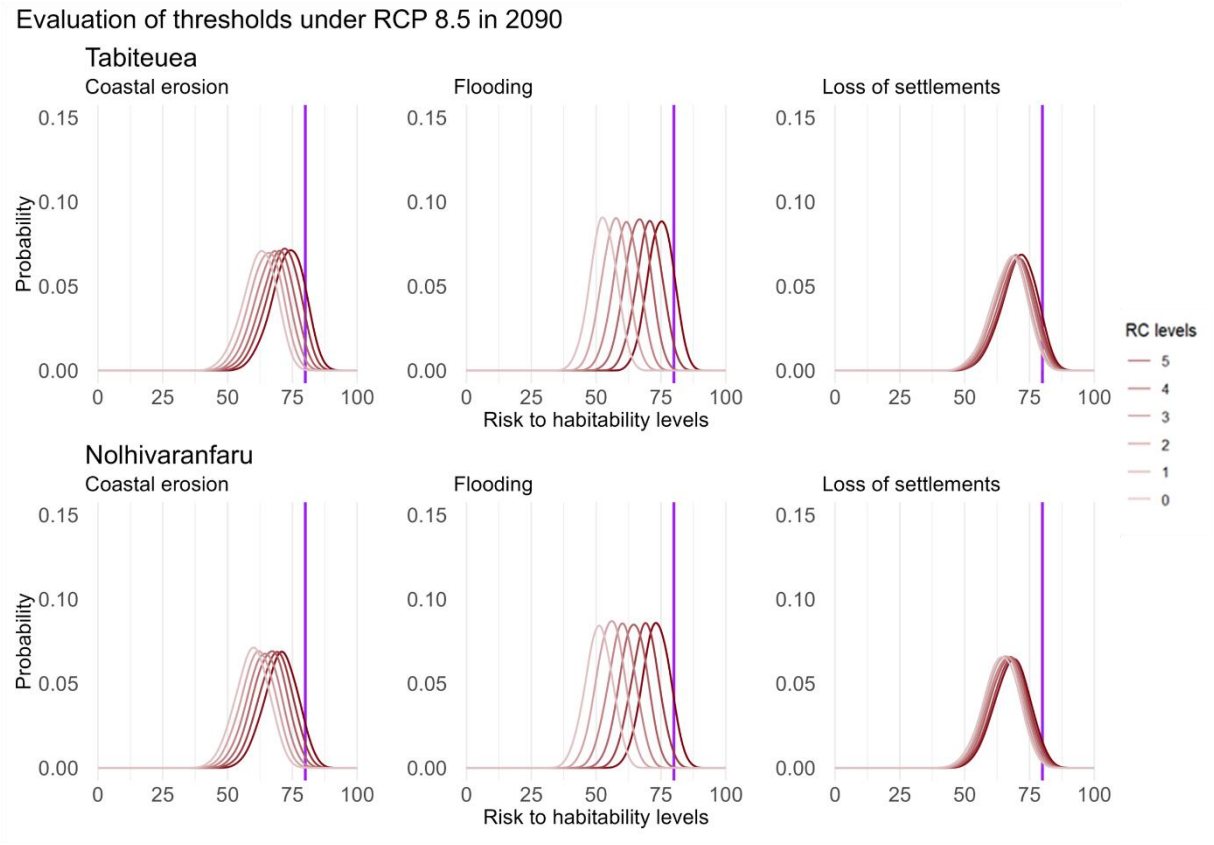

Figure S4 Risk to Tabiteuea and Nolhivaranfaru habitability under the RCP 8.5 in 2090. Each distribution represents the impact of different risk criteria levels. For example, for a flooding risk of 1, the query is written as P(Risk to habitability | RCP = 8.5 & Time = 2090 & Flooding = 1). The results suggest that in both atoll islands, severe risk criteria could lead to reaching adaptation limits (purple line).

S2.2. Identification of major drivers of risks: Which risk factors are present when the risk to island habitability is high or very high?

In this analysis, we explore the conditions that lead to high or very high risk to habitability, by calculating the probability of each risk criteria level when the risk to habitability is high or very high. This probability was calculated under the RCP 8.5 in 2090.

Figure S5 shows the results for Male'. The probability distributions with and without the constraint of high risk to habitability are represented by red and gray bars respectively. Under a high risk to habitability, the most likely risk criteria levels are 4 and 5, indicating a correlation with severe risk criteria. This is the case for multiple variables including *flooding*, *loss of settlements*, *loss of critical infrastructures*, and *transport connectivity*. The variations between the distributions with and without the habitability constraint reflect the impact of the risk to habitability node on the risk criteria nodes and vice-versa. For example, with the habitability constraint, we can observe a shift in the distribution of *flooding*, which reflects the impact of this risk factor on the risk to habitability.

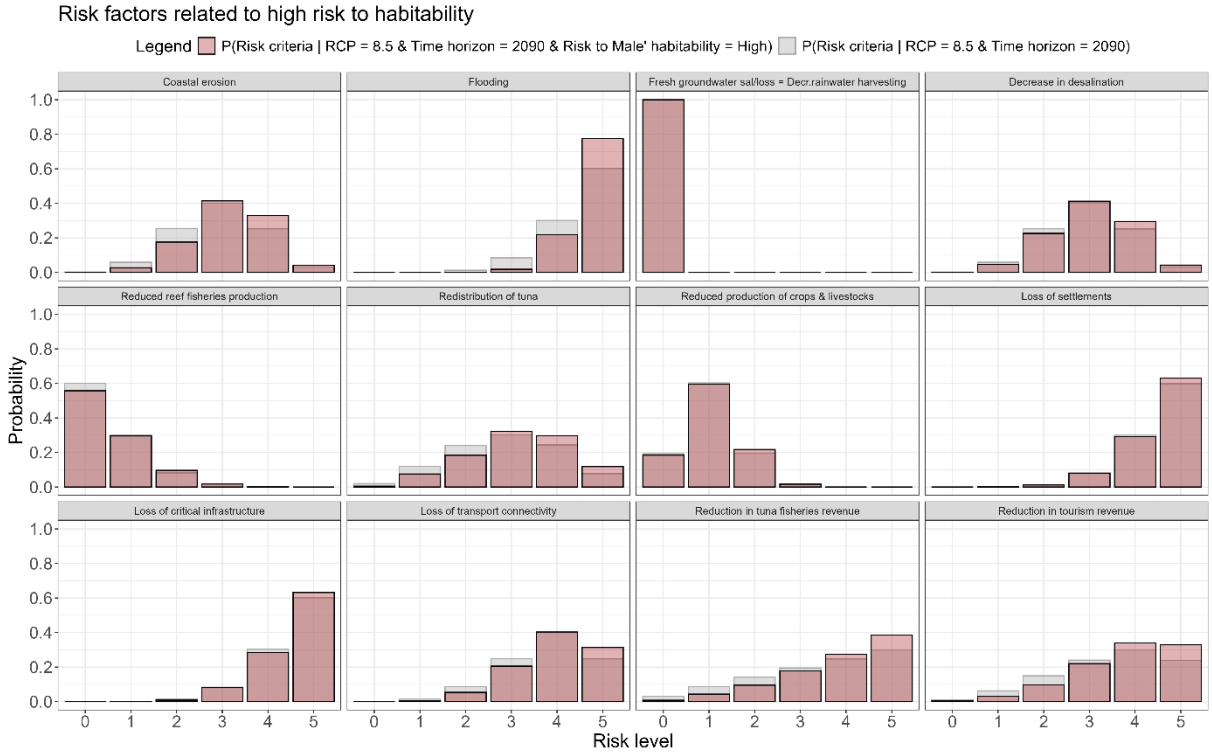

Figure S5 Probability of risk criteria under the RCP 8.5 in 2090. The red bars represent the results when the risk to Male' habitability is high (query: P(Risk criteria | RCP = 8.5 & Time horizon = 2090 & Risk to Male' habitability = High)). The grey bars represent the results without the habitability constraint (query: P(Risk criteria | RCP = 8.5 & Time horizon = 2090)). The results reflect which risk criteria are related to high risk to habitability. These risk criteria include flooding, loss of critical infrastructure, and loss of settlements.

Figure S6 shows the results for Tabiteuea. In this atoll island, we observe the same correlation between high risk to habitability with severe risk criteria. This is the case for *flooding, coastal erosion, reduced reef fisheries production*, and *loss of settlements* and *critical infrastructures*. With the habitability constraint we can observe a significant shift in the distribution of *flooding*, *coastal erosion*, and *reduced reef fisheries production*, which reflects the impact of these risk factors on the risk to habitability.

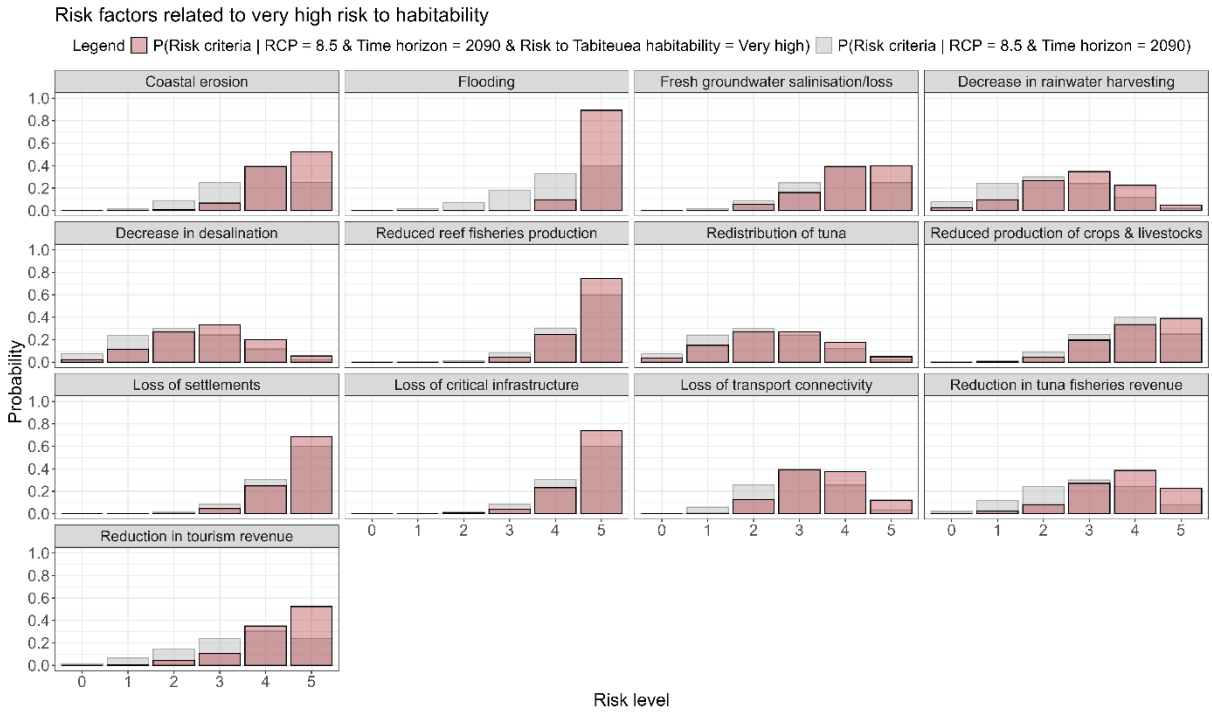

Figure S6 Probability of risk criteria levels under the RCP 8.5 in 2090. The red bars represent the results when the risk to Tabiteuea habitability is very high (query: P(Risk criteria | RCP = 8.5 & Time horizon = 2090 & Risk to Tabiteuea habitability = Very high)). The grey bars represent the results without the habitability constraint (query: P(Risk criteria | RCP = 8.5 & Time horizon = 2090)).

Figure S7 shows the results for Nolhivaranfaru. In this atoll island, when the risk to habitability is very high, the most likely outcomes are severe risk criteria including *flooding*, *coastal erosion*, *loss of settlements and critical infrastructures*, *loss of transport connectivity*, and *reduction in tourism revenue*. With the habitability constraint, we can observe a significant shift in the distribution of *flooding*, *coastal erosion*, and *redistribution of tuna*, which reflects the impact of these risk factors on the risk to habitability.

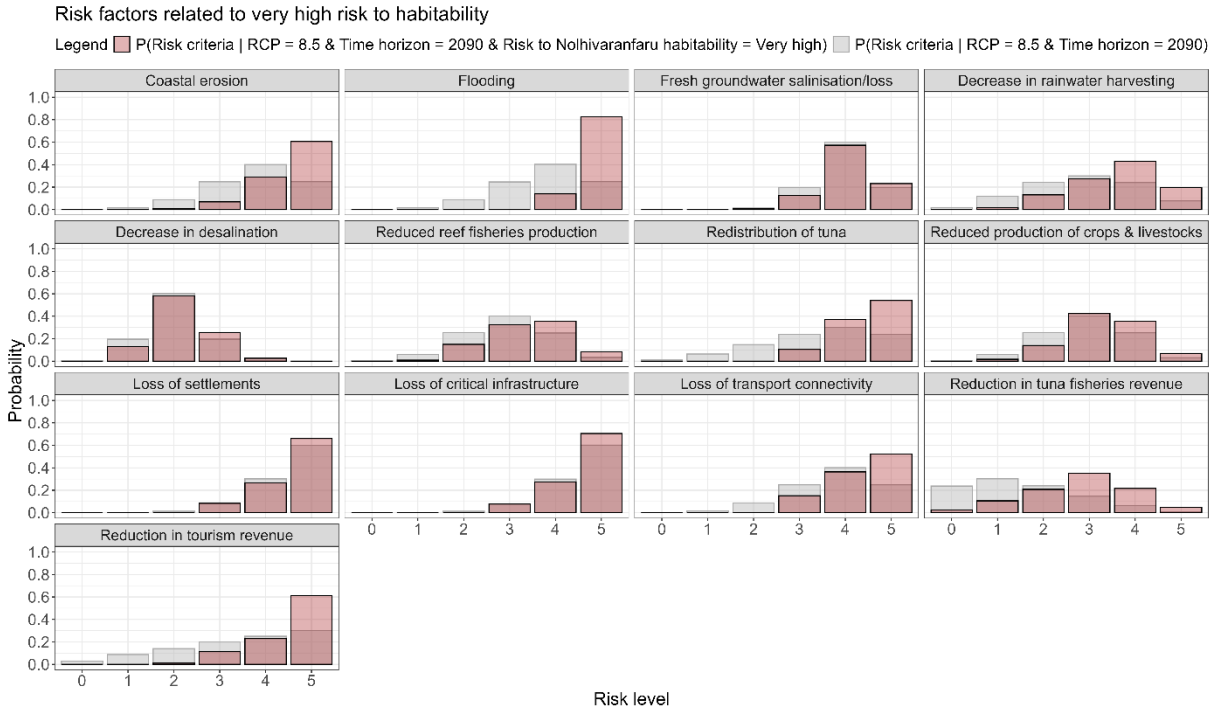

Figure S7 Probability of risk criteria levels under the RCP 8.5 in 2090. The red bars represent the results when the risk to Nolhivaranfaru habitability is very high (query: P(Risk criteria | RCP = 8.5 & Time horizon = 2090 & Risk to

Nolhivaranfaru habitability = Very high)). The grey bars represent the results without the habitability constraint (query: P(Risk criteria | RCP = 8.5 & Time horizon = 2090)).

S2.3. Effectiveness of adaptation measures: How much is the risk to habitability reduced if we act on the risk factors that contribute the most?

In this section, we assess the impact of adaptation measures in Tabiteuea and Nolhivaranfaru. Figure S8 shows the probability of the risk to habitability given a risk criteria level <= 2 under the RCP = 8.5 in 2090. In both atoll islands, the results show that reducing *flooding* has a major impact on the risk to habitability. These outcomes also suggest that a combination of adaptation measures is needed to reduce the risk to habitability from high to moderate.

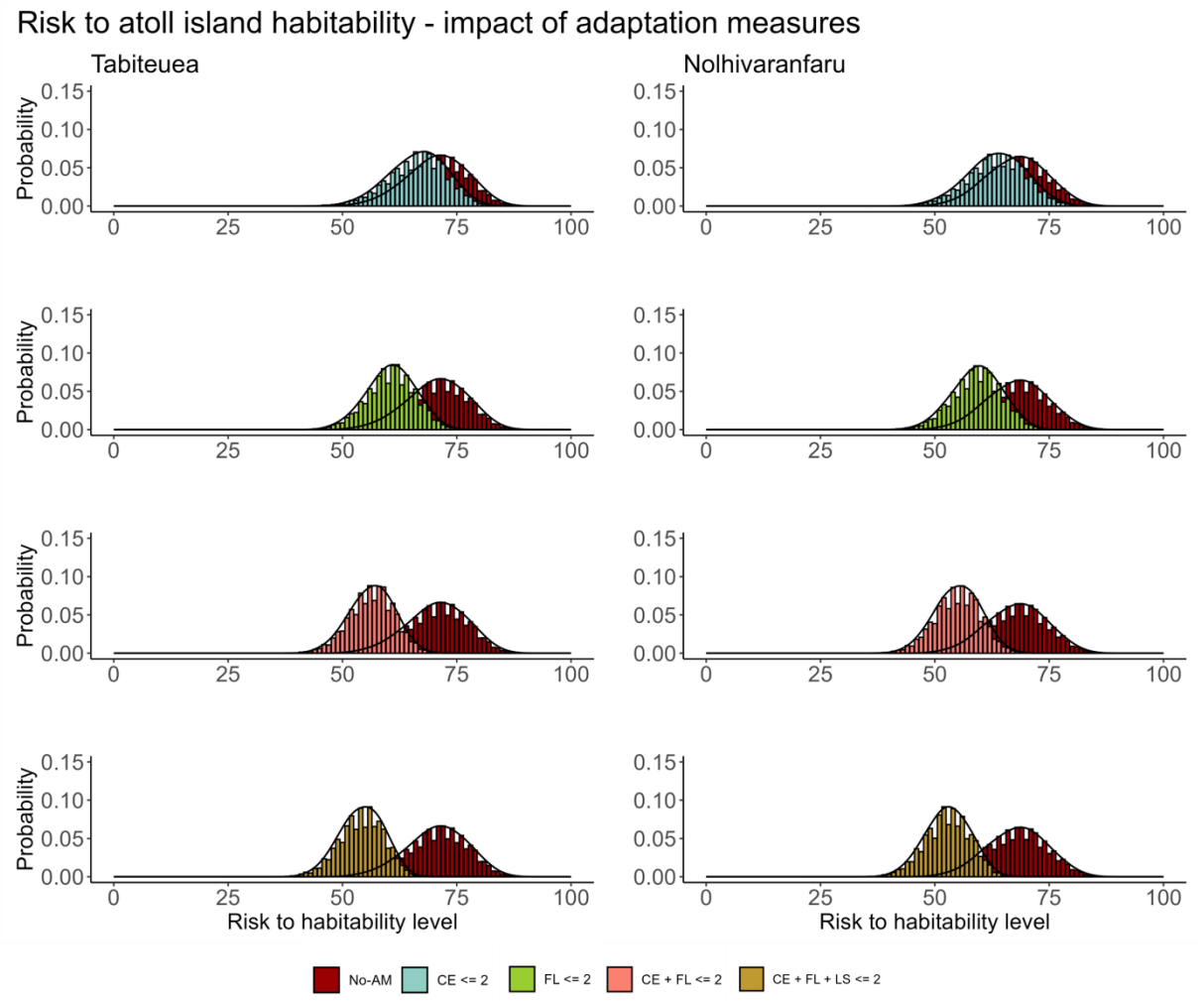

Figure S8 Probability distributions of the risk to habitability given different adaptation measures under RCP 8.5 in 2090 in Tabiteuea and Nolhivaranfaru.

S2.4. Likely ranges from BN risk assessment

The BN allows to quantify the confidence by providing the 17*th* and 83*rd* percentile results (Figure S9). The interval is interpreted as the likely range, to refer to a probability of at least 66%, according to the IPCC likelihood scale.

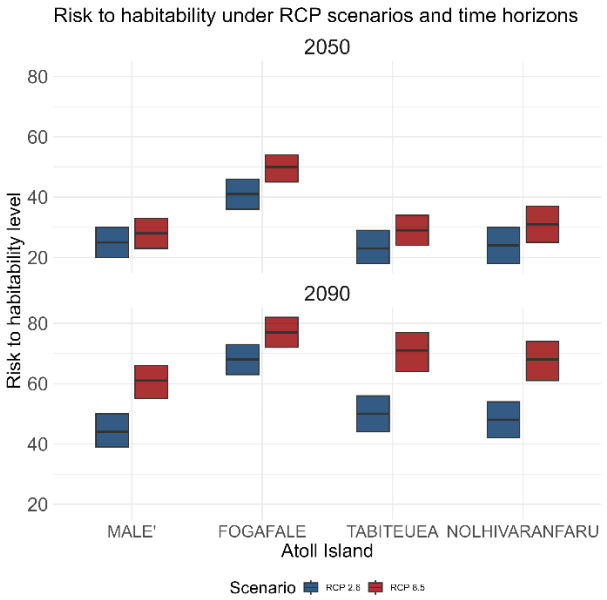

Figure S9 Median and likely range [17th – 83rd percentile] of the risk to habitability. Blue bars represent the results for RCP 8.5 and red bars for RCP 2.6.

S3. Sensitivity test

This supplement supports section 5.3 of the main manuscript.

We carried out a sensitivity test to evaluate the impact of our conditions. We generated an alternative set of Beta distributions (Figure S10) satisfying another set of conditions shown in Table S2. In this case, we associated a higher weight to the confidence levels, resulting in less dispersed distributions.

Table S2 Conditions for the alternative set of Beta distributions.

Confidence level	Probability weight (case 2)	Standard deviation
1	40%	0.20
2	60%	0.15
3	80%	0.10
4	90%	0.05
5	100% (Dirac)	-

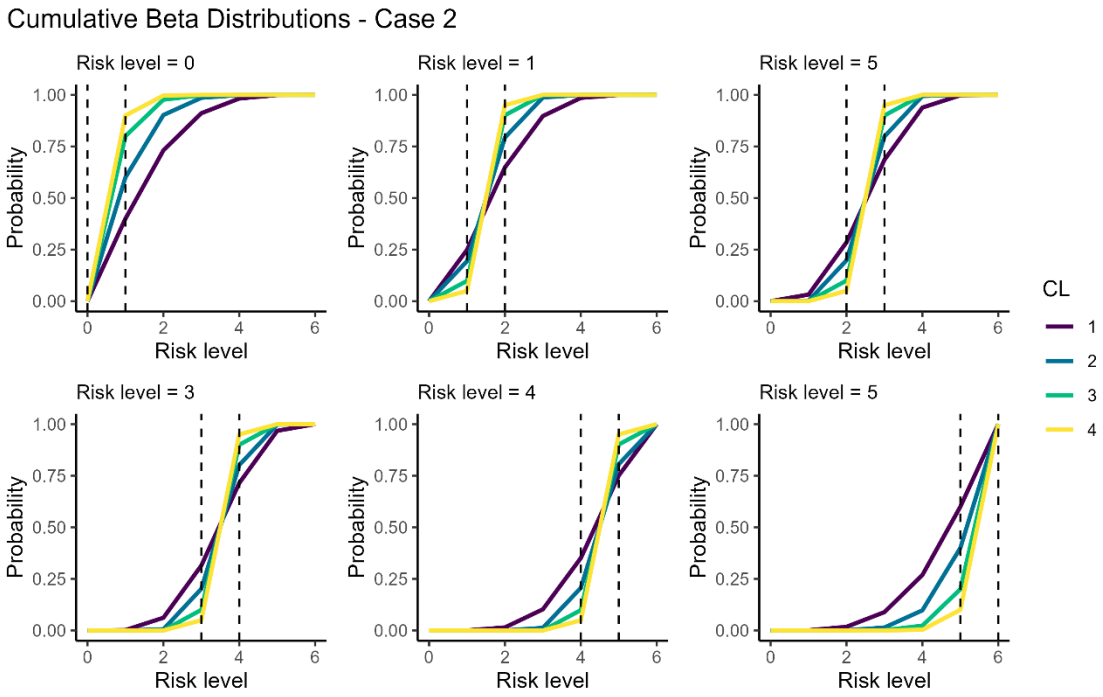

Figure S10 Alternative set of Beta distributions.

S3.2. Sensitivity test results: risk assessment

Figure S11 shows the risk assessment results using the alternative set of Beta distributions. In this case, the probability distributions are less dispersed and the medians are slightly different (Table S3). However, in all atoll islands, the most likely risk level is the same as that estimated using the initial set of Beta distributions.

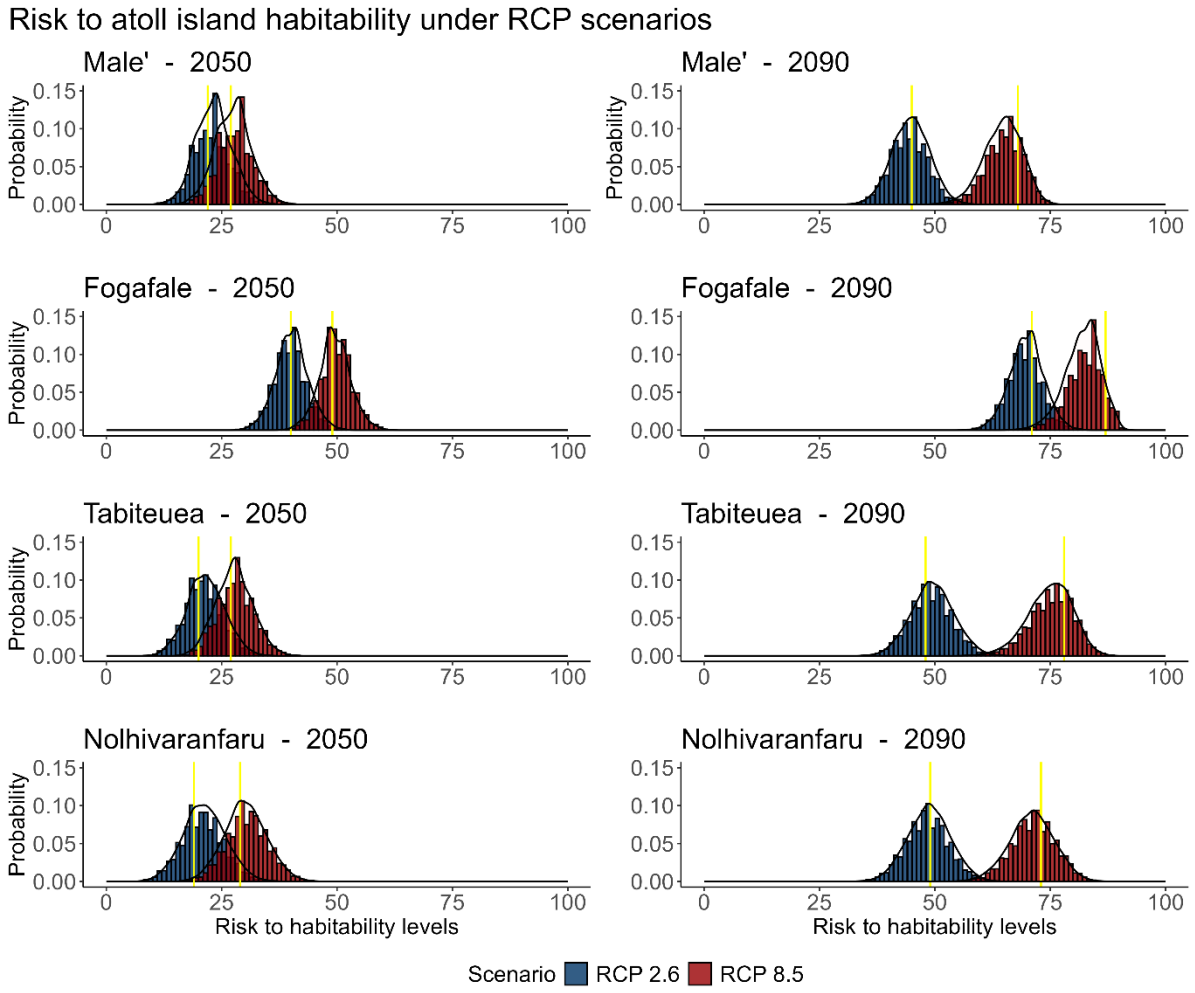

Figure S11 Results of the risk to habitability assessment using the alternative set of Beta distributions. The results show less dispersed distributions. However, using the initial and the alternative set, we obtain the same risk categories for all scenarios.

Table S3 Results showing the risk to habitability for the RCP 2.6 and 8.5 scenarios in 2050 and 2090.

2050	**Aggregated risk level (Duvat et al.,2021)**		**Case 1: Risk level range Median [17th to 83rd percentiles]**		**Case 2: Risk level range Median [17th to 83rd percentiles]**	
Atoll island	**RCP 2.6**	**RCP 8.5**	**RCP 2.6**	**RCP 8.5**	**RCP 2.6**	**RCP 8.5**
Male’	22	27	25[20-30]	28[23-33]	23[19-26]	27[23-31]
Fogafale	40	49	41[36-46]	50[45-54]	40[36-43]	49[46-52]
Tabiteuea	20	27	23[18-29]	29[24-34]	21[17-25]	27[23-31]
Nolhivaranfaru	19	29	24[18-30]	31[25-37]	21[17-25]	30[25-34]
2090						
Male’	45	68	44[39-50]	61[55-66]	44[41-48]	64[60-68]
Fogafale	71	87	68[63-73]	77[72-82]	69[66-73]	82[78-85]
Tabiteuea	48	78	50[44-56]	71[64-77]	49[45-53]	75[70-79]
Nolhivaranfaru	49	73	48[42-54]	68[61-74]	48[44-53]	71[66-75]

S3.3. Sensitivity test results: identification of critical thresholds

We explored the possibility of atoll islands to reach adaptation limits using the alternative set of Beta distributions. These limits are related to the purple zone on burning embers diagrams, which show the changes in risk to humans

and ecosystems as a function of global mean temperature (Zommers et al., 2020). The purple zone in these diagrams indicates a very high risk that can cause irreversible impacts and exceedance of adaptation limits. In this work, a very high risk is represented by risk to habitability > 80 (purple line). The results are very similar to those obtained using the initial set (Table S4). Under RCP 8.5 in 2090 in Male', the results suggest that no risk criteria level could lead to exceeding the adaptation threshold. Conversely, under the same scenario in Fogafale severe risk criteria levels may lead to exceeding this limit (Figure S12).

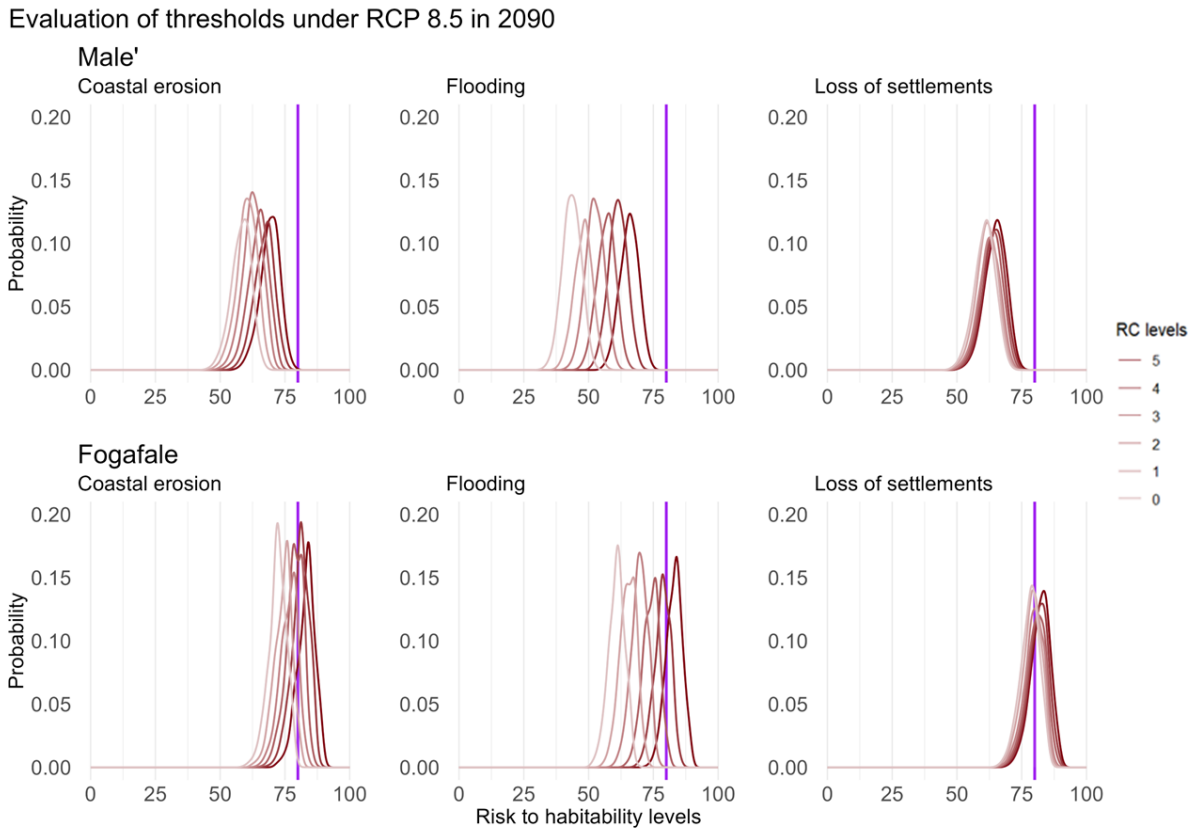

Figure S12 Probability distributions of the risk to habitability given different risk criteria levels using the alternative set of Beta distributions. Example of query: P(Risk to habitability | RCP = 8.5 & Time = 2090 & Coastal erosion = 2).

Table S4 Likely range and median values of the risk to habitability given different risk criteria levels under the RCP 8.5 in 2090 for Male' and Fogafale.

Male' RCP 8.5 2090	**Median [17th to 83rd percentiles]**					
Risk level	**Coastal erosion**		**Flooding**		**Loss of settlements**	
	Case 1	**Case 2**	**Case 1**	**Case 2**	**Case 1**	**Case 2**
0	54[49-59]	58[54-61]	41[36-45]	43[40-46]	57[51-62]	61[56-64]
1	57[51-61]	60[56-63]	45[40-50]	48[44-51]	58[52-63]	61[57-65]
2	59[53-64]	62[58-66]	50[45-54]	52[48-55]	59[53-64]	62[58-66]
3	61[56-66]	65[61-68]	54[49-59]	57[53-60]	60[54-65]	63[59-67]
4	63[58-68]	67[63-70]	63[58-68]	61[57-64]	60[55-66]	64[60-67]
5	66[60-70]	69[65-72]	51[57-62]	65[62-69]	61[56-67]	65[60-68]
Fogafale RCP 8.5 2090	**Median [17th to 83rd percentiles]**					
Risk level	**Coastal erosion**		**Flooding**		**Loss of settlements**	
	Case 1	**Case 2**	**Case 1**	**Case 2**	**Case 1**	**Case 2**
0	68[63-72]	72[68-75]	57[53-61]	61[57-63]	73[68-78]	78[74-81]

1	70[65-75]	74[70-77]	61[57-66]	65[62-68]	74[69-79]	79[75-82]
2	73[68-77]	76[73-79]	66[61-70]	69[66-72]	75[70-80]	80[76-83]
3	75[70-79]	78[75-82]	70[66-75]	74[71-77]	76[70-81]	80[77-84]
4	77[72-81]	81[77-84]	75[70-79]	78[75-81]	77[71-82]	81[77-84]
5	79[74-84]	83[79-86]	79[75-83]	83[79-86]	78[72-82]	82[78-85]

S3.4. Sensitivity test results: identification of major risk factors

We analysed the conditions that lead to a very high risk to habitability using the second set of Beta distributions. Figure S13 shows the probability distributions with (red) and without (gray) the constraint of very high risk to habitability. Using the initial and the alternative set, we identified the same risk criteria leading to very high risk conditions. Under a very high risk to habitability, the most likely levels are levels 4 and 5, indicating a correlation with severe risk criteria. These risk criteria include a *decrease in rainwater harvesting* and *desalination*, severe *flooding* and *coastal erosion, reduced fisheries production*, and *loss of settlements, critical infrastructures, and transport connectivity*.

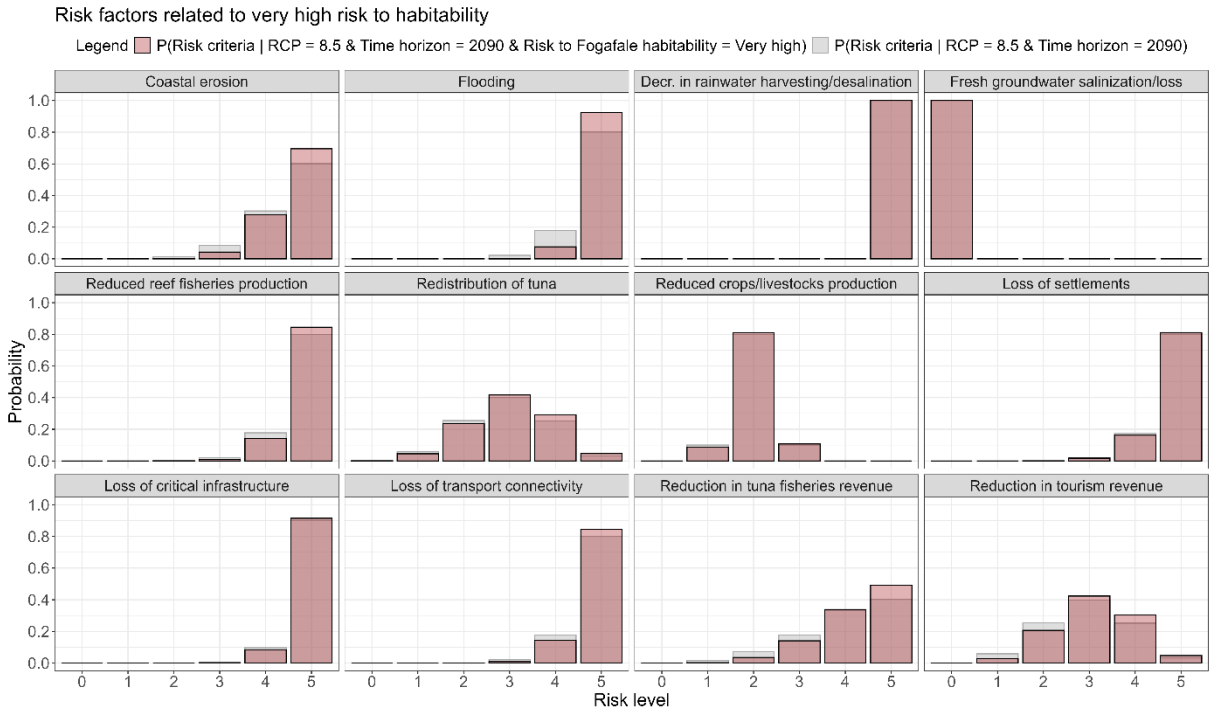

Figure S13 Probability of risk criteria levels under the RCP 8.5 in 2090 using the alternative set of Beta distributions. The red bars show the results when the risk to habitability is very high (query: P(Risk criteria | RCP = 8.5 & Time horizon = 2090 & Risk to Fogafale habitability = Very high)). The grey bars represent the results without the habitability constraint (query: P(Risk criteria | RCP = 8.5 & Time horizon = 2090)).

S3.5. Sensitivity test results: effectiveness of adaptation measures

Finally, we evaluated the impact of adaptation measures using the second set of Beta distributions (Figure S14). The probability distributions are less dispersed and present slight median variations (Table S5). However, in all atoll islands, the most likely risk level remains the same as that estimated using the initial set of Beta distributions.

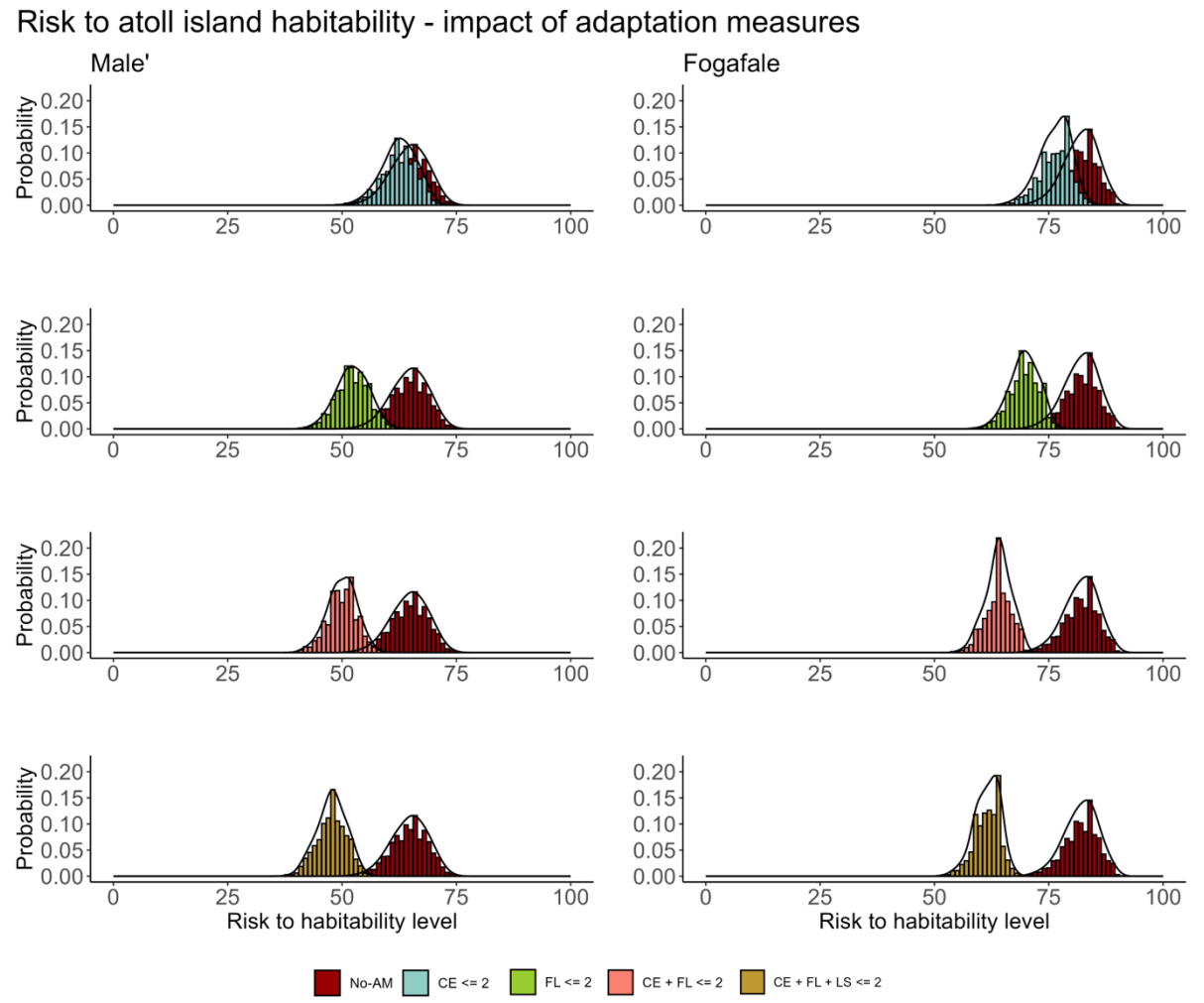

Figure S14 Probability distributions of the risk to habitability given different adaptation measures under RCP 8.5 in 2090 in Male' and Fogafale. These results were generated using the alternative set of Beta distributions. In this case, we observed less dispersed distributions and small median variations. However, the most likely risk level is the same as that estimated using the initial set of Beta distributions.

Table S5 Likely range and median values for the risk to habitability given different adaptation measures using the alternative set of Beta distributions.

Atoll island	**Risk to habitability range - Median [17th to 83rd percentiles]** **CE = Coastal erosion FL = Flooding LS = Loss of settlements**							
	CE		**FL**		**CE + FL**		**CE + FL + LS**	
	Case 1	Case 2	Case 1	Case 2	Case 1	Case 2	Case 1	Case 2
Male'	58[53-63]	62[58-66]	50[45-54]	52[48-55]	47[42-51]	50[47-53]	45[40-49]	47[44-50]
Fogafale	72[67-77]	76[73-79]	66[61-70]	69[66-72]	61[56-64]	64[61-66]	59[54-62]	61[58-64]

References

Duvat, V. K. E., Magnan, A. K., Perry, C. T., Spencer, T., Bell, J. D., Wabnitz, C. C. C., Webb, A. P., White, I., McInnes, K. L., Gattuso, J.-P., Graham, N. A. J., Nunn, P. D., and Le Cozannet, G.: Risks to future atoll habitability from climate-driven environmental changes, WIREs Climate Change, 12, e700, https://doi.org/10.1002/wcc.700, 2021.

Zommers, Z., Marbaix, P., Fischlin, A., Ibrahim, Z. Z., Grant, S., Magnan, A. K., Pörtner, H.-O., Howden, M., Calvin, K., Warner, K., Thiery, W., Sebesvari, Z., Davin, E. L., Evans, J. P., Rosenzweig, C., O'Neill, B. C., Patwardhan, A., Warren, R., van Aalst, M. K., and Hulbert, M.: Burning embers: towards more transparent and robust climate-change risk assessments, Nature Reviews Earth & Environment, 1, 516–529, https://doi.org/10.1038/s43017-020-0088-0, 2020.